SUPPLEMENTARY INFORMATION

I. HOPPER FLOW

The discharge of grains from a hopper or silo has received considerable attention, both because it is relevant to numerous industries, and a model system for examining general features of granular flow [1, 2]. These studies have generally focused on the motion of grains inside the hopper and the flow rate of material out of the nozzle. It is known that these systems can exhibit intermittent jamming and density waves which could potentially effect clustering. To check that the details of the nozzle flow do not govern the cluster formation, we performed experiments with both cylindrical and conical nozzles, nozzles with smooth and rough walls, and externally vibrated the nozzle. We observed nearly identical clusters in all cases.

The nozzle and reservoir are the same as described in [3]. Briefly, a 9 cm diameter resevior of grains feeds a nozzle which consists of a porous, 13 cm long, 16 mm diameter cylinder with flat disk at the base containing a circular aperture. Due to the Janssen effect, these dimensions guarantee a steady flow rate provided the reservoir is sufficiently full [4, 5]. The mean velocity of grains leaving the nozzle u_0 varies with the diameter of the opening D_0, from 0.15 m/s for $D_0 = 1$ mm to 0.25 m/s for $D_0 = 6$ mm, roughly independent of grain diameter or material. After leaving the nozzle, the grains accelerate under gravity so the downward velocity grows with depth z as $u(z) = \sqrt{u_0^2 + 2gz}$, causing the stream to elongate and stretch as it falls. While the stream is stretching due to gravity it simultaneously thins, which is evident in the images of the stream near the nozzle. The average diameter of the stream decays with depth as $D(z) \sim D_0(1 + 2gz/u_0^2)^{-1/4}$ so that $u(z)D(z)^2 \sim$ constant. This implies that the packing density of the stream remains roughly constant as the stream falls.

II. AIR DRAG

Interactions between grains and air can have profound on effects on the flow of granular materials, particularly in fine grains [6–8]. It is possible for air to affect the granular stream, either by disrupting the flow out of the nozzle or through drag on the grains as they fall. However, we find that air has little effect on the clustering observed here, in agreement with previous studies [3, 9].

It is known that granular flow out of nozzle can be disrupted by the back-flow of air into the nozzle, leading to an oscillatory 'ticking' flow [10]. As described in [3], this is eliminated in our experiments by using porous wire mesh for the nozzle walls, which allows the gas pressure in the nozzle to equilibrate and eliminates the back flow of air. We confirmed this by checking that the flow rate is independent of gas pressure.

To illustrate the role of air drag on the free-falling stream, we show the breakup of a granular stream in air at atmospheric pressure (Fig. 1a-d). Despite the larger drag force on the grains, the initial formation of the clusters is unaffected. The undulations appear at the same point below the nozzle, and the clusters are nearly identical in size and shape to clusters formed in vacuum. The only significant difference is that the increased air drag at atmospheric pressure rips grains off the edges of the stream, causing the clusters to break up further downstream. This faster disintegration of the clusters in air was also described in [3], while Khamontoff briefly noted that the clusters appeared more regular at a vacuum of 4 kPa [9].

In Fig. 1e,f we plot the drag force F_D on a single $d = 100$ μm grain as a function of both ambient pressure P_0 and velocity u, using both dilute gas [11] and finite Reynolds number corrections to Stokes law [12]. For a single, isolated grain in free fall this drag force slows its acceleration until it reaches a terminal velocity u_T and the drag force balances the weight of the grain. For a 100 μm grain, this terminal velocity is ~ 0.5 m/s at 101 kPa, and ~ 5.0 m/s at 0.03 kPa. By contrast, the dense stream velocity reaches over 6 m/s at the bottom of the 200 cm fall, well above the terminal velocity for a single grain. Any grain removed from the stream will therefore rapidly decelerate, moving upwards from the free-falling reference frame. For this to happen, the air must overcome the cohesive forces between the grains.

At atmospheric pressure (101 kPa), the air drag almost immediately exceeds the measured range of cohesive forces between grains F_{coh} (10 - 40 nN for untreated glass), allowing drag to easily rip grains off the stream. At our lowest

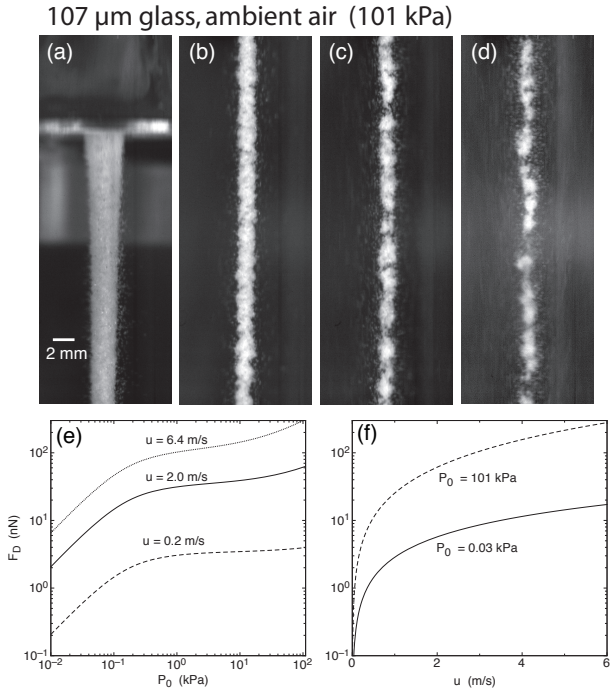

FIG. 1: Effect of air drag. (a) - (d) Stream of $d = 107$ μm glass grains falling under atmospheric air pressure (101 kPa) at conditions otherwise identical to those in Fig. 1a-d in the main article. Images are shown (a) just below the nozzle, (b) z = 20 cm, (c) 55 cm and (d) 97 cm from the top of the frame to the nozzle. e,f Drag force on a single 100 μm grain as a function of pressure (e) and as a function of velocity (f). Using $u(z) = \sqrt{u_0^2 + 2gz}$, with $u_0 \simeq 0.2$ m/s, the three curves in e correspond to $z = 0$ cm (0.2 m/s), $z = 20$ cm (2.0 m/s) and $z = 200$ cm (6.4 m/s). The drag force is calculated according to $F_D = F_S(1 + 0.15Re^{0.687})(1 + K(a + be^{-c/K})^{-1}$, where $F_S = 3\pi\eta du$ is the Stokes drag, the first factor is a correction for finite Reynolds number $Re = \rho ud/\eta$ [12] and the second factor is a correction for the drag at low pressures [11], which depends on the Knudsen number $K = 2L_{mfp}/d$. The viscosity of air $\eta = 1.8 \times 10^{-5}$ Pa s is independent of pressure. The density of the ambient air is $\rho \propto P_0$, which at 101 kPa is 1.2 kg/m^3. The mean free path of air is $L_{mfp} \propto 1/P_0$ and at 101 kPa is roughly 68 nm. The empirical constants $a = 0.86$, $b = 0.29$ and $c = 1.25$ are taken from [11].

accessible vacuum (0.03 kPa), the drag is lower by roughly a factor of 10 and remains well below the range of cohesive forces until the velocity reaches about 4 m/s, which occurs at a depth of about $z = 100$ cm. As the stream continues to fall, F_D continues to increase, so even in vacuum some grains will fly off the stream below a depth of about 100 cm. This is indeed what we observe experimentally (see supplementary movies). The removal of grains from the stream can therefore be used to estimate the cohesion between grains mentioned in the main text.

III. ELECTROSTATIC EFFECTS

In addition to van der Waals and capillary forces, electrostatic forces are a potential source of cohesion between grains [13, 14]. It is well known that electrostatic charging can occur when two materials are brought into contact or rubbed against each other, though the details of this process are not completely understood [15]. This tribocharging is most commonly seen between different types of materials, but it can also occur spontaneously between identical insulators [16, 17].

To examine the importance of electrostatic forces, we directly measure the charge on the grains by subjecting the stream to an electric field. For these experiments, the stream passes between two large, 30 cm x 30 cm aluminum plates spaced 9 cm apart. A voltage between 1 kV - 18 kV is applied across the plates, creating a strong, uniform electric field perpendicular to the stream (Fig. 2e). Charged grains fly off the stream nearly symmetrically toward both plates, indicating the presence of grains with positive and negative net charges. This suggests that the dominant source of charging is from grains colliding with each other, as opposed to grains colliding with the container walls. Using $F = qE$ for the horizontal force and accounting for the air drag on the individual grains, we can estimate the

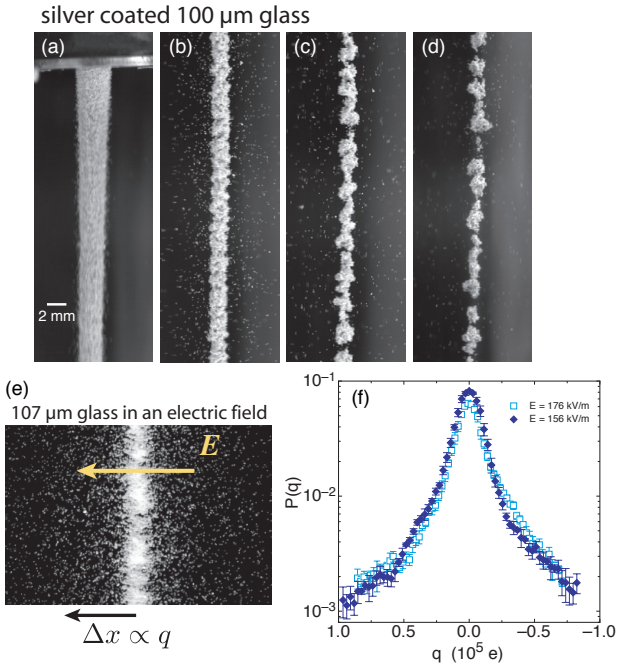

FIG. 2: Electrostatic effects. (a) - (d) Stream of conductive, silver-coated $d = 100$ μm glass grains. Conditions are otherwise identical to those in Fig. 1a-d in the main paper. Images are shown (a) just below the nozzle, (b) $z = 20$ cm, (c) 55 cm and (d) 97 cm from the top of the frame to the nozzle. e, A stream of 107 μm glass grains in an uniform 200 kV/m electric field directed perpendicular to the stream, as indicated by the arrow. Charged grains fly off the stream uniformly in both directions, indicating both positive and negative net charges on the stream. f, Distribution of charges $P(q)$ on a stream of glass grains. A thinner, more diffuse stream is used to calculate $P(q)$ in order to minimize charge transfer between grains in contact, though this does not substantially change $P(q)$. Open and closed symbols show charge distributions measured using two different field strengths.

charge of grains pulled away from the stream from the distribution of displacements Δx from the center of the stream [18]. These charged grains account for a small fraction of all the grains inside the stream, with a maximum net charge corresponding to roughly $\pm 100,000$ electrons (Fig. 2f). Nevertheless, even at this maximum net charge the attractive force is only 0.1 nN from Coulomb's law, assuming a separation of 100 μm. From this we conclude that electrostatic forces are too small to be the dominant source of cohesion.

We note that the copper grains used in our experiments are oxidized and not conducting. To further check that electrostatic forces are not important in driving the observed clustering, we performed experiments with conductive silver-coated 100 μm glass grains and observed identical clusters to those in the untreated glass (Fig. 2 a-d).

IV. GRAIN SHAPE AND ROUGHNESS

As noted in the main text, in addition to the grain mass and cohesive force between grains, clustering is also affected by the grain shape. Figure 3 shows how the clustering changes when glass spheres are replaced by nearly identically sized coarse sand ($d = 110 \pm 30$ μm, US Silica F110). There is no substantial change in the nozzle velocity or the initial profile of the stream near the nozzle (Fig. 3a). As the stream falls, undulations appear, but the undulations are less regular and develop into tenuous, diffuse clusters compared to the compact clusters seen in glass spheres (Figs. 3b-d). This places the rough sand on the borderline between clustering (like clean glass) and not clustering (like clean copper). SEM images of the different materials (Fig. 3 e-g) show that the coarse sand is rougher and more irregular than both the glass and copper. The cohesive forces F_{coh} between sand grains are similar to those between clean glass and the mass of the sand grains and the glass is nearly identical, so the difference between the compact and tenuous clusters must arise from differences in the collisions between the smooth and rough grains.

The scenario for clustering proposed in the main paper only considers simple, 'sticky' collisions of grains and neglects sliding or rolling dissipation; however to completely describe a collision, one must consider both the normal

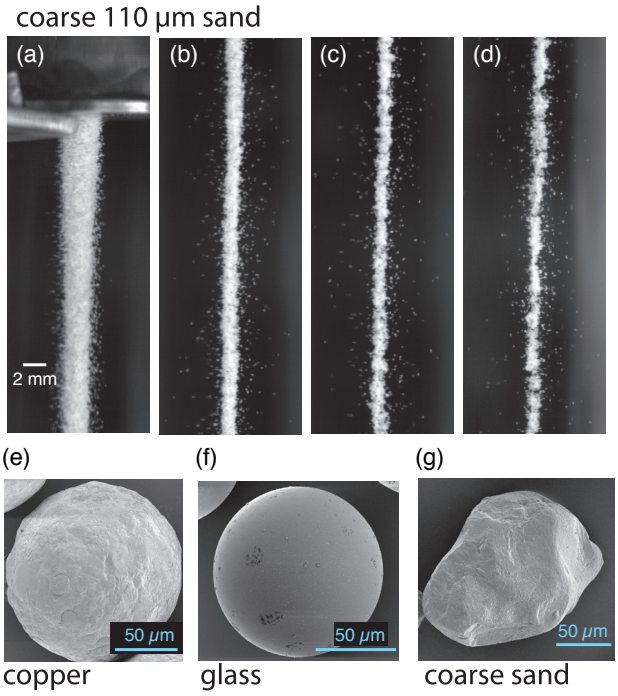

FIG. 3: Effect of grain shape. (a) - (d) Stream of coarse $d = (110 \pm 30)$ μm sand (US Silica F110). Conditions are otherwise identical to those in Fig. 1a-d in the main paper. Images are shown (a) just below the nozzle, (b) $z = 20$ cm, (c) 55 cm and (d) 97 cm from the top of the frame to the nozzle. e-g, Representative SEM images of a copper grain (e) a glass grain (f) and a coarse sand grain (g).

and tangential forces[19]. In general one expects sliding motion for smooth spheres and a reversal of the tangential motion for extremely rough spheres. However, even for spherical grains with small asperities (such as glass Fig. 3f), the forces governing the tangential motion can be complicated and depend on the surface roughness, as well as on the normal and tangential impact velocity [20]. For grains with larger asperities that encompass a significant fraction of the grain radius, such as copper and coarse sand (Figs. 3e,g), collisions are even more complicated, since tangential motion can directly be transfered into normal motion. One way for grain shape to reduce clustering is by slowing the initial inelastic cooling, keeping the kinetic granular temperature larger than the work required to overcome cohesion, W_{coh}. It is also possible that W_{coh} is reduced in irregular grains, for example by reducing sliding motion and hence reducing the the effective distance over which cohesive forces act.

It is important to separate the effects of overall grain shape from those of nano-scale surface roughness, which directly affects the cohesive forces between grains, F_{coh}. Adding nanoscale asperities to the 150 μm glass grains reduced the cohesive force between grains by roughly a factor of two and significantly reduced clustering. AFM topographic images and line scans (Fig. 4) show that this increase in roughness is only apparent on a scale below 100 nm (Fig. 4f), making it very different from the large scale roughness features seen in copper grains and coarse sand. Therefore, the absence of clustering in the Aerosil coated glass is a direct consequence of the reduced cohesive force between grains.

[1] Jaeger, H. M., Nagel, S. R. & Behringer, R. P. Granular solids, liquids, and gases. *Rev. Mod. Phys.* **68**, 1259–1273 (1996).
[2] Duran, J. *Sands, powders, and grains: an introduction to the physics of granular materials* (Springer-Verlag, New York, 200).
[3] Möbius, M. E. Clustering instability in a freely falling granular jet. *Phys. Rev. E* **74**, 051304 (2006).
[4] Janssen, H. A. Versuche über Getreidedruck in silozellen. *Zeitschr. d. Vereines deutscher Ingenieure* **39**, 1045 – 1049 (1895).
[5] Nedderman, R. M., Tüzün, U., Savage, S. B. & Houlsby, G. T. The flow of granular materials - I : Discharge rates from

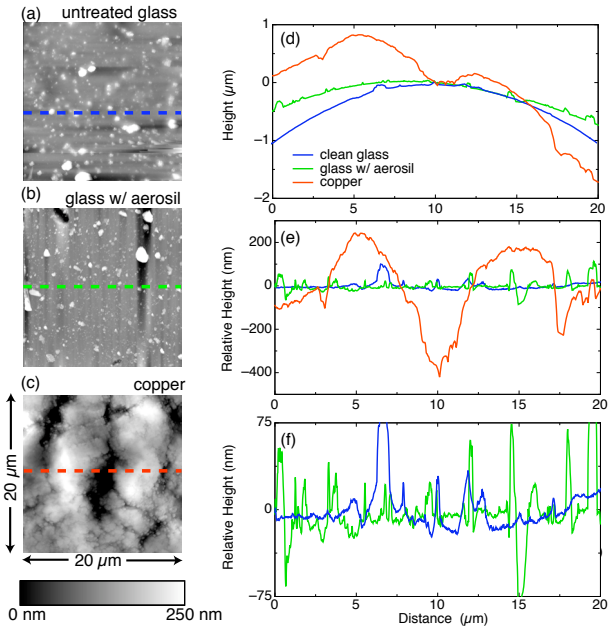

FIG. 4: Grain topography. a-c, AFM topographic maps of a 20 μm $\times$ 20 μm section of a glass grain (a), a glass grain coated with aerosil (b) and a copper grain (c). To highlight asperities and roughness, the images have been flattened to remove the global curvature of the grains. Over the full 20 μm $\times$ 20 μm sections, the root mean square (RMS) roughness is 39 nm (glass), 46 nm (glass w/ aerosil) and 125 nm (copper). d-f, Line scans taken along the dashed lines in each of the images (a-c) showing the raw surface profile (d) and relative surface profile after flattening (e,f). The scans in (f) are the same data for glass also shown in (e), but with expanded vertical scale.

hoppers. *Chemical Engineering Science* **37**, 1597–1609 (1982).
[6] Pak, H. K., Van Doorn, E. & Behringer, R. P. Effects of ambient gases on granular materials under vertical vibration. *Phys. Rev. Lett.* **74**, 4643–4646 (1995).
[7] Möbius, M. E., Lauderdale, B. E., Nagel, S. R. & Jaeger, H. M. Brazil-nut effect: Size separation of granular particles. *Nature* **414**, 270–270 (2001).
[8] Royer, J. R. *et al.* Formation of granular jets observed by high-speed x-ray radiography. *Nature Physics* **1**, 164–167 (2005).
[9] Khamontoff, N. Application of photography to the study of the structure of trickles of fluid and dry materials. *J. Russ. Physico-Chm. Soc. Saint Petersburg* **22**, 281 (1890).
[10] Wu, X.-l., Måløy, K. J., Hansen, A., Ammi, M. & Bideau, D. Why hour glasses tick. *Phys. Rev. Lett.* **71**, 1363–1366 (1993).
[11] Milikan, R. A. The general law of fall of a small spherical body through a gas, and its bearing upon the nature of molecular reflection from surfaces. *Phys. Rev.* **22**, 1–23 (1923).
[12] Schiller, L. & Nauman, A. A drag coefficient correlation. *V.D.I. Zeitung* **77**, 318 (1935).
[13] Visser, J. Van der waals and other cohesive forces affecting powder fluidization. *Powder Technol.* **58**, 1–10 (1989).
[14] Podczeck, F. *Particle-particle Adhesion in Pharmaceutical Powder Handling* (Imperial College Press, London, 1998).
[15] Schein, L. B. Recent progress and continuing puzzles in electrostatics. *Science* **316**, 1572–1573 (2007).
[16] Lowell, J. & Truscott, W. S. Triboelectrification of identical insulators: I. an experimental investigation. *J. Phys. D: Appl. Phys* **19**, 1273–1280 (1986).
[17] Shinbrot, T., Komatsu, T. & Zhao, Q. Spontaneous tribocharging of similar materials. *Europhys. Lett.* **83**, 24004 (2008).
[18] Schein, L. B., LaHa, M. & Marshall, G. Electrostatic charging of two insulating powders. *J. Appl. Phys.* **69**, 6817–6826 (1991).
[19] Brilliantov, N. V. & Pöschel, T. *Kinetic Theory of Granular Gases* (Oxford Graduate Texts. Oxford University Press, Oxford, 2004).
[20] Brilliantov, N. V., Spahn, F., Hertzsch, J.-M. & Pöschel, T. Model for collisions in granular gases. *Phys. Rev. E* **53**, 5382–5392 (1996).